Ancient TL

www.ancienttl.org · ISSN: 2693-0935

Roberts, R., Yoshida, H., Galbraight, R., Lastett, G., Jones, R. and Smith, M., 1998. *Single-aliquot and single-grain optical dating confirm thermoluminescence age estimates from Malakunanja II rock shelter in northern Australia.* Ancient TL 16(1): 19-24.
https://doi.org/10.26034/la.atl.1998.287

Single-aliquot and single-grain optical dating confirm thermoluminescence age estimates at Malakunanja II rock shelter in northern Australia

Richard Roberts[1], Hiroyuki Yoshida[1], Rex Galbraith[2], Geoff Laslett[3], Rhys Jones[4] and Mike Smith[5]

[1] Department of Earth Sciences, La Trobe University, Melbourne, VIC 3083, Australia
[2] Department of Statistical Science, University College London, London WC1E 6BT, UK
[3] CSIRO Mathematical and Information Sciences, Melbourne, VIC 3168, Australia
[4] Department of Archaeology and Natural History, Research School of Pacific and Asian Studies, Australian National University, Canberra, ACT 0200, Australia
[5] People and Environment Section, National Museum of Australia, Canberra, ACT 2601, Australia

(Received 3 May 1998 ; in final form 22 May 1998)

Introduction

The earliest direct ages for human occupation of Australia are 50–60 ka from Malakunanja II and Nauwalabila I rock shelters in the Northern Territory (Roberts, 1997). These ages were obtained from unheated quartz sediments using thermoluminescence (TL) dating at Malakunanja II (Roberts *et al.*, 1990a, 1990b) and optical dating at Nauwalabila I (Roberts *et al.*, 1994). At both sites, a combination of additive-dose and regenerative-dose multiple-aliquot procedures was used to estimate the palaeodoses, while the dose rates were determined principally from high-resolution gamma-ray spectrometry analyses (which showed that a condition of secular equilibrium presently exists in the ^{238}U and ^{232}Th chains).

The reliability of TL dating methods for some rock shelter deposits has since been thrown into doubt by TL ages of more than 100 ka reported for human occupation of the Jinmium site in north-western Australia (Fullagar *et al.*, 1996). It has been suggested, however, that the high TL ages at Jinmium are the result of insufficient exposure to sunlight of some grains before burial (Roberts, 1997; Spooner, 1998). This suggestion has now been confirmed by optical dating of individual quartz grains and by ^{14}C dating of charcoal fragments, the conclusion being that the entire deposit was formed in the last 10 ka (Roberts *et al.*, 1998).

We have now examined quartz grains from two key samples (KTL162 and KTL164) from Malakunanja II (Figure 1) and found that single-grain optical ages, multiple-grain optical ages, and TL ages agree at this site, thereby confirming the original age estimates.

Sampling and dating procedures

Sample KTL162 was collected from the same level as the lowest artefact and produced a TL age of 61 ± 10 ka. Sample KTL164 was taken from the level immediately overlying a small pit containing artefacts and gave a TL age of 45 ± 7 ka. Details of site stratigraphy, sample preparation, TL dating methods, and dose rate determinations have been published previously (Roberts *et al.*, 1990a, 1990b). In the original study, the random and systematic age uncertainties were summed arithmetically; here they are added in quadrature, following standard practice (Aitken, 1985: Appendix B).

The optical dating apparatus, methods and statistical models employed here follow those used in the Jinmium study (Roberts *et al.*, 1998). Palaeodoses were estimated using a single-aliquot regenerative-dose protocol, in which sensitivity is monitored by measuring the optically stimulated luminescence (OSL) induced by a small test dose applied after measuring each of the natural and regenerated OSL signals (Murray and Roberts, 1998; Murray and Mejdahl, submitted). The palaeodoses were divided by the published dose rates (0.77 ± 0.09 Gy ka^{-1} for

KTL162, and 0.91 ± 0.08 Gy ka^{-1} for KTL164; Roberts *et al.*, 1990a) to obtain the optical ages.

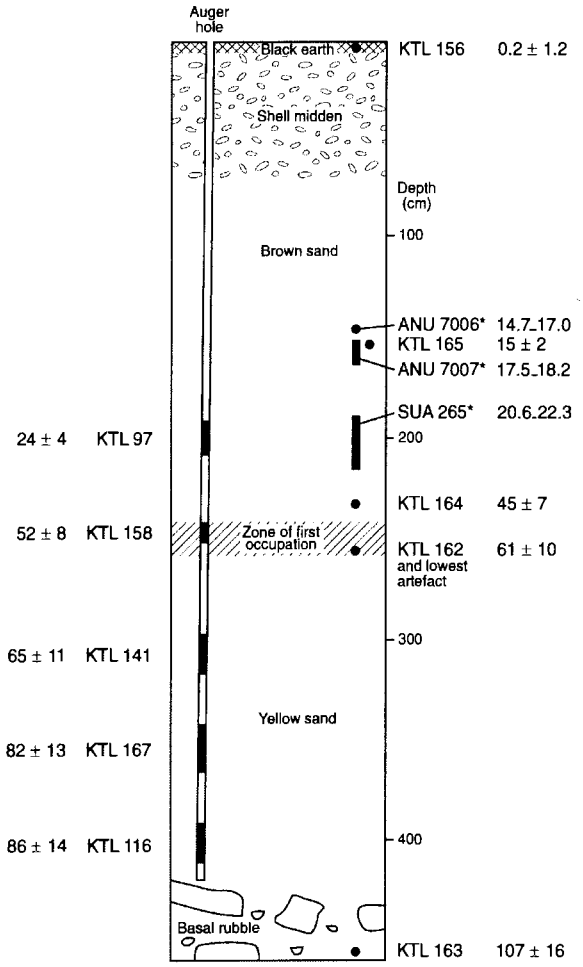

Figure 1.
Stratigraphic section of the Malakunanja II excavation (south-west face), showing the locations, depth intervals, and ages (in thousands of years) of the TL and ^{14}C samples. The three ^{14}C samples are marked by an asterisk. TL ages are given as mean age ± 1σ total uncertainty, while the calibrated (Stuiver and Reimer, 1993) ^{14}C ages are shown as 2σ age ranges.

Single-aliquot measurements

Optical dating was first applied to 24 aliquots of sample KTL162 and 24 aliquots of sample KTL164, with each aliquot being composed of many (~800) quartz grains of 90–125 μm diameter (the size fraction used also in the TL study). The dose (palaeodose) received by the mineral grains since their last exposure to sunlight was estimated for each aliquot using a range of preheat temperatures (160–300°C for 10s), test doses of 0.5 Gy, and a regenerative dose of 47 Gy (KTL162) or 42 Gy (KTL164).

Palaeodoses were constant with preheat temperature for both KTL162 (Figure 2) and KTL164, which we interpret as indicating negligible thermal transfer (except from traps responsible for the 110°C TL peak). The average palaeodose (for all 24 aliquots) was calculated for KTL162 (46.7 ± 1.2 Gy) and for KTL164 (41.5 ± 1.0 Gy), and these yielded ages of 60.7 ± 7.5 ka and 45.7 ± 4.1 ka, respectively.

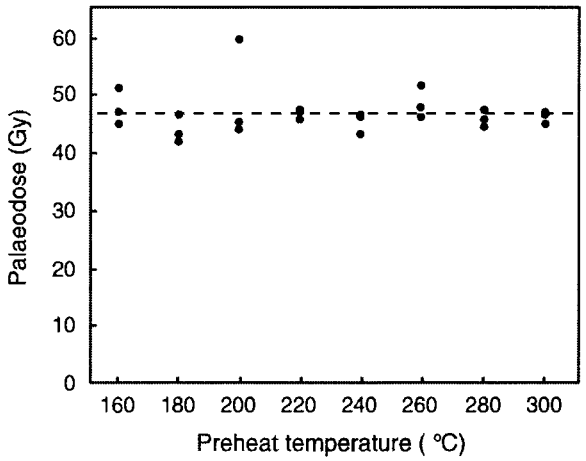

Figure 2.
Palaeodoses obtained from 24 aliquots of sample KTL162 at different preheat temperatures using a regenerative-dose protocol. Three aliquots were held for 10 s at each preheat temperature. Each aliquot was composed of ~800 grains and was stimulated for 100 s at 125°C. The uncertainty in palaeodose estimation (1σ level) for each aliquot is smaller than the size of the symbol. The plateau from 160°C to 300°C implies negligible thermal transfer, except from traps responsible for the 110°C TL peak (Murray and Roberts, 1998). The average palaeodose is marked by the dashed line.

Single-grain measurements

Palaeodoses were then estimated for 85 and 86 individual grains from KTL162 and KTL164, respectively, using a preheat of 270°C (KTL162) or 260°C (KTL164) for 10 s, test doses of 1 Gy, and a regenerative dose of 47 Gy (KTL162) or 42 Gy (KTL164). Palaeodoses were calculated using the measured natural, regenerative dose, and test dose OSL signals specific to each grain. The test dose signals were measured for each grain to correct for any change in sensitivity between the natural and regenerative dose cycles. Consequently, grains with

weak test dose signals yielded palaeodoses with correspondingly large relative errors.

Most of the 85 grains from KTL162 have palaeodoses of 30–50 Gy and none have significantly larger palaeodoses (the latter might indicate the presence of insufficiently bleached grains). One grain has a significantly smaller palaeodose (~16 Gy) and this grain is presumed to have intruded from the overlying deposits. Most grains were weakly luminescent and only 18 of them produced significant test dose signals (i.e. where the rate of luminescence decay during the first few seconds of optical stimulation was statistically greater than zero at the 2σ level). Figure 3(a) is a radial plot (see 'Discussion') of the palaeodoses determined for these 18 grains; the numerical values are given in the Appendix, together with the sensitivity changes monitored using the test dose signals.

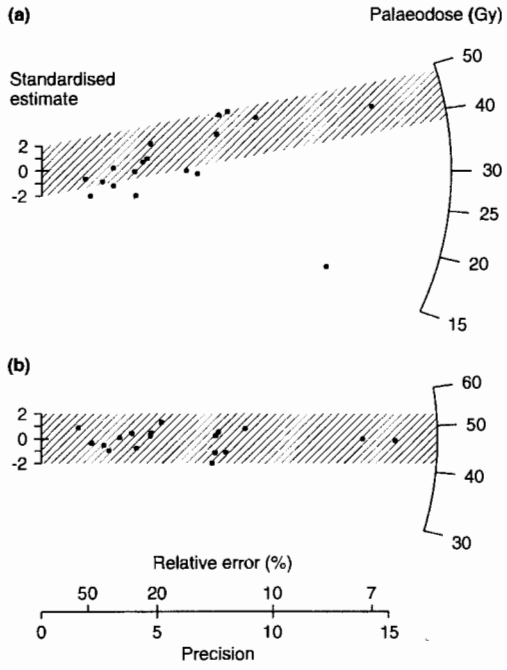

Figure 3.
(a) *Radial plot of palaeodoses determined for 18 individual grains (those with statistically significant test dose signals) from sample KTL162 using a regenerative-dose single-aliquot optical dating protocol. Single grains vary in luminescence intensity, resulting in differing palaeodose precisions. The y-axis plots standardised estimates of log palaeodose, given by log palaeodose minus a central value (log 30 Gy in this example), divided by the standard error of log palaeodose. The x-axis (precision) plots reciprocal standard errors of log palaeodose; these may be converted to approximate relative errors of palaeodose, which are also shown. Points on any straight line radiating from the origin have the same log palaeodose; a circular scale has been added so that palaeodoses (log scale) may be read off. For grains with the same true log palaeodose, 95% of the points should lie within ± 2 units (on the y-axis) of a common radial line, as shown by the hatched component centered at 42.7 Gy which corresponds to the estimate of central palaeodose (see 'Discussion'). Further details on radial plots are given by Galbraith (1988, 1990, 1994).*

(b) *Radial plot of the doses calculated for the same 18 individual grains plotted in (a) after bleaching each grain with 420–550 nm light (for 125 s at 125°C) and then giving a laboratory beta dose of 47 Gy to each grain. The hatched component is centered at the applied dose of 47 Gy and it can be seen that all points are statistically concordant with this dose.*

Each of the 85 grains from KTL162 was then given a second regenerative dose and a third test dose, and the regenerative-dose protocol was run again: the correct (known) dose was obtained for all grains, as illustrated in Figure 3(b) for the 18 grains with statistically significant test dose signals. This figure shows that all points are consistent with the applied dose of 47 Gy, taking into account their measurement errors. This experimental check is reassuring, although it does not account for heterogeneity in the beta dose rate that may occur in a field context and that could introduce an additional source of variation to the palaeodose values calculated for single grains buried at the same time.

Sample KTL164 showed a similar pattern of single-grain palaeodoses: most of the 86 grains have palaeodoses of 30–50 Gy, none have significantly larger palaeodoses, and one grain has a significantly smaller palaeodose (~19 Gy). The general consistency of palaeodose estimates for single grains from samples KTL162 and KTL164 implies a lack of significant post-depositional disturbance of the Malakunanja II sediments, indicating that artefacts are unlikely to have intruded into these levels.

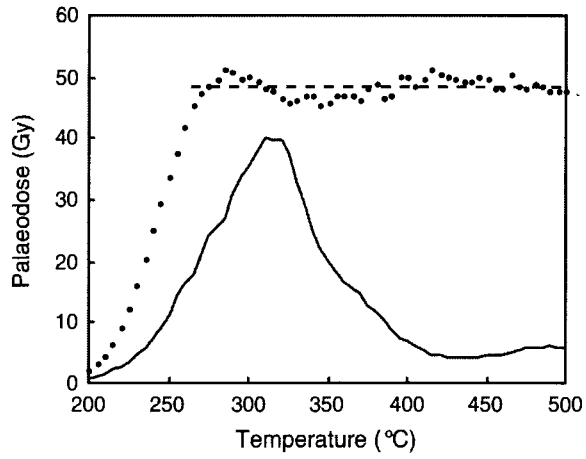

Figure 4.
TL palaeodose versus temperature plot for sample KTL162. Palaeodoses were determined by the total-bleach method (see Roberts et al., 1990a for experimental details). Palaeodose uncertainties (1σ level) are typically ± 10% or better, and the average palaeodose (~48 Gy) across the plateau region (270–500°C) is marked by the dashed line. The solid line shows the TL glow curve for a natural aliquot. Roberts et al. (1990a) present similar data for sample KTL164.

Discussion

A radial plot (Galbraith, 1988, 1990, 1994), rather than a histogram, has been used to plot single-grain palaeodoses because the precisions associated with palaeodose measurements differ considerably between grains due to their varying luminescence intensities. It is not appropriate to plot such palaeodoses on a histogram because a histogram takes no account of their varying precisions, and the inclusion of relatively imprecise points could seriously distort the frequency distribution. However, a histogram may be used to display points that have similar and high precisions, such as the palaeodoses calculated for single aliquots composed of multiple grains.

Application of a central-age model (modified from Galbraith and Laslett, 1993) to grains from KTL162 with high-precision palaeodoses (those with relative errors of ± 20% or better, excluding the ~16 Gy grain) gives a central palaeodose of 42.7 ± 3.6 Gy and an age of 55.5 ± 8.2 ka. Each estimate is quoted with ± 1 standard error, which represents the usual 68% confidence interval. A similar procedure applied to KTL164 (to the 12 grains with high-precision palaeodoses, excluding the ~19 Gy grain) yields a central palaeodose of 40.2 ± 2.3 Gy and an age of 44.2 ± 4.7 ka. The central palaeodose is an estimate of the geometric mean of the true (i.e. in the absence of measurement error) single-grain palaeodoses.

An additional parameter of interest is the dispersion of single-grain palaeodose populations. This parameter measures the relative standard deviation of the palaeodoses in the absence of measurement errors, so it indicates dispersion over and above the measurement error associated with each grain (following Galbraith and Laslett, 1993). In Figure 3(b), for example, all points are consistent with a common palaeodose of 47 Gy and the dispersion parameter is estimated to be zero.

For each of the two samples KTL162 and KTL164 (those grains with high-precision palaeodoses, excluding the ~16 Gy and ~19 Gy grains), the dispersion parameter is estimated to be ~17%. The relative standard deviation of the measured palaeodoses will be higher and will differ between grains, because each has an associated measurement error, and is about 18–26% for these samples. This estimate is similar in magnitude to the empirical relative standard deviation of 21–27% reported for the single-grain palaeodoses at Allen's Cave (Murray and Roberts, 1997). But all of these estimates of dispersion are somewhat uncertain because they are based on small numbers of grains.

Heterogeneity in beta dosimetry was considered to be the most likely explanation for the palaeodose dispersion at Allen's Cave (Murray and Roberts, 1997) because the deposit contains a mixture of quartz sand, carbonate, and aeolian silt and clay with strongly contrasting beta dose rates (Olley *et al.*, 1997). The Malakunanja II deposit, however, is composed of siliceous sands that are apt to exhibit much less variation in beta microdosimetry. We might therefore expect the Malakunanja II samples to have smaller palaeodose dispersions than the Allen's Cave sample, but further data are needed to permit a definitive comparison.

We are also further investigating the issue of post-depositional disturbance by selecting grains of larger diameter (200–2,000 μm) to profit from three potential advantages. First, larger grains may be less easily displaced by ground water percolation and by the small-scale activities of soil fauna, thereby minimising the number of intrusive grains encountered at any level within the deposit. Second, if luminescence intensity is approximately proportional to grain volume then 200–2,000 μm-diameter grains

should be 10–10,000 times brighter than 100 μm-diameter grains, so that appreciable test dose signals are produced by a greater proportion of individual grains. And third, the beta contribution to the total dose rate will be reduced for larger grains because of significant beta attenuation, and this should produce a correspondingly reduced dispersion in single-grain palaeodoses when the dispersion is caused by variations in beta microdosimetry.

Conclusions

These single-aliquot and single-grain optical dating results support our earlier TL-based findings that people were present in Australia at 50–60 ka. They also show that correct burial ages can be obtained using TL methods, provided the sediments are bleached sufficiently before burial to reset the dating signal. The Jinmium sediments failed to meet this requirement (Roberts, 1997; Spooner, 1998), whereas adequate bleaching at Malakunanja II is indicated by the modern TL age for the near-surface sample (Figure 1), the similarity of palaeodoses obtained from TL signals (at 325°C and 375°C) with markedly different susceptibilities to light (Figure 4), and the concordance of TL and ^{14}C ages at this site (Figure 1). Optical dating of single grains also provides a means of testing for significant post-depositional disturbance of rock shelter sediments.

Acknowledgements

We thank Jon Olley and Martin Aitken for comments on a draft on this manuscript. CSIRO Mathematical and Information Sciences kindly supported R.G. in Australia, and R.R. is supported by a Queen Elizabeth II Fellowship from the Australian Research Council.

References

Aitken, M.J. (1985). *Thermoluminescence Dating*. Academic Press, London.

Fullagar, R.L.K., Price, D.M. and Head, L.M. (1996). Early human occupation of northern Australia: archaeology and thermoluminescence dating of Jinmium rock-shelter, Northern Territory. *Antiquity* **70**, 751-773.

Galbraith, R.F. (1988). Graphical display of estimates having differing standard errors. *Technometrics* **30**, 271-281.

Galbraith, R.F. (1990). The radial plot: graphical assessment of spread in ages. *Nuclear Tracks and Radiation Measurements* **17**, 207-214.

Galbraith, R.F. (1994). Some applications of radial plots. *Journal of the American Statistical Association* **89**, 1232-1242.

Galbraith, R.F. and Laslett, G.M. (1993). Statistical models for mixed fission track ages. *Radiation Measurements* **21**, 459-470.

Murray, A.S. and Mejdahl, V. (submitted). Comparison of regenerative-dose single-aliquot and multiple-aliquot (SARA) protocols using heated quartz from archaeological sites. *Quaternary Science Reviews* (submitted).

Murray, A.S. and Roberts, R.G. (1997). Determining the burial time of single grains of quartz using optically stimulated luminescence. *Earth and Planetary Science Letters* **152**, 163-180.

Murray, A.S. and Roberts, R.G. (1998). Measurement of the equivalent dose in quartz using a regenerative-dose single-aliquot protocol. *Radiation Measurements* (in press).

Olley, J.M., Roberts, R.G. and Murray, A.S. (1997). Disequilibria in the uranium decay series in sedimentary deposits at Allen's Cave, Nullarbor Plain, Australia: implications for dose rate determinations. *Radiation Measurements* **27**, 433-443.

Roberts, R.G. (1997). Luminescence dating in archaeology: from origins to optical. *Radiation Measurements* **27**, 819-892.

Roberts, R.G., Jones, R. and Smith, M.A. (1990a). Thermoluminescence dating of a 50,000 year-old human occupation site in northern Australia. *Nature* **345**, 153-156.

Roberts, R.G., Jones, R. and Smith, M.A. (1990b). Stratigraphy and statistics at Malakunanja II: reply to Hiscock. *Archaeology in Oceania* **25**, 125-129.

Roberts, R.G., Jones, R., Spooner, N.A., Head, M.J., Murray, A.S. and Smith, M.A. (1994). The human colonisation of Australia: optical dates of 53,000 and 60,000 years bracket human arrival at Deaf Adder Gorge, Northern Territory. *Quaternary Science Reviews* **13**, 575-583.

Roberts, R., Bird, M., Olley, J., Galbraith, R., Lawson, E., Laslett, G., Yoshida, H., Jones, R., Fullagar, R., Jacobsen, G. and Hua, Q. (1998). Optical and radiocarbon dating at Jinmium rock shelter in northern Australia. *Nature* **393**, 358-362.

Spooner, N.A. (1998). Human occupation at Jinmium, northern Australia: 116,000 years ago or much less? *Antiquity* **72**, 173-178.

Stuiver, M. and Reimer, P.J. (1993). Extended ^{14}C data base and revised CALIB 3.0 ^{14}C age calibration program. *Radiocarbon* **35**, 215-230.

Appendix

Numerical values for the 18 individual grains from sample KTL162 that gave statistically significant test dose signals (see 'Single-grain measurements'). Columns 2 to 4 list the palaeodoses and 1σ uncertainties, as plotted in Figure 3(a). Columns 5 to 7 list the ratios and 1σ uncertainties of the regenerative/natural test dose signals.

Grain number	Palaeodose (Gy)	Standard error (Gy)	Relative error (%)	Test R / Test N	Standard error (Gy)	Relative error (%)
5	32.4	10.6	33	0.89	0.29	32
19	30.1	4.8	16	0.96	0.15	16
22	53.8	7.1	13	1.14	0.15	13
25	54.3	6.8	13	1.19	0.15	12
28	29.7	7.4	25	1.05	0.26	25
30	21.5	8.3	39	1.29	0.49	38
34	20.4	6.7	33	1.14	0.36	31
35	21.3	11.4	54	0.45	0.24	54
50	29.0	4.3	15	1.12	0.16	15
54	18.4	4.6	25	1.06	0.26	24
62	11.4	5.5	48	0.93	0.44	47
67	35.4	8.2	23	0.72	0.16	23
70	16.0	1.3	8	1.36	0.11	8
99	47.6	5.2	11	0.76	0.08	11
105	44.2	5.9	13	1.10	0.14	13
107	43.1	3.0	7	0.91	0.06	7
109	37.4	8.3	22	0.96	0.21	22
110	47.8	10.3	21	1.14	0.24	21

Reviewer

M.J. Aitken